Heliyon 10 (2024) e37319

Contents lists available at ScienceDirect

Heliyon

journal homepage: www.cell.com/heliyon

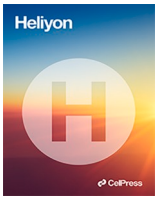

Research article

Genetic patterning in hippocampus of rat undergoing impaired spatial memory induced by long-term heat stress

Peihua Long [a,1], Qunfei Ma [a,1], Zhe Wang [a], Guanqin Wang [a], Jianan Jiang [a], Lu Gao [a,b,*]

[a] Department of Physiology, Naval Medical University, Shanghai, 200433, PR China
[b] Shanghai Key Laboratory for Assisted Reproduction and Reproductive Genetics, Shanghai, 200120, PR China

ARTICLE INFO

Keywords:
Long-term heat stress
Spatial memory
Hippocampus
Neuron
Arhgap36

ABSTRACT

The organism's normal physiological function is greatly impacted in a febrile environment, leading to the manifestation of pathological conditions including elevated body temperature, dehydration, gastric bleeding, and spermatogenic dysfunction. Numerous lines of evidence indicate that heat stress significantly impacts the brain's structure and function. Previous studies have demonstrated that both animals and humans experience cognitive impairment as a result of exposure to high temperatures. However, there is a lack of research on the effects of prolonged exposure to high-temperature environments on learning and memory function, as well as the underlying molecular regulatory mechanisms. In this study, we examined the impact of long-term heat stress exposure on spatial memory function in rats and conducted transcriptome sequencing analysis of rat hippocampal tissues to identify the crucial molecular targets affected by prolonged heat stress exposure. It was found that the long-term heat stress impaired rats' spatial memory function due to the pathological damages and apoptosis of hippocampal neurons at the CA3 region, which is accompanied with the decrease of growth hormone level in peripheral blood. RNA sequencing analysis revealed the signaling pathways related to positive regulation of external stimulation response and innate immune response were dramatically affected by heat stress. Among the verified differentially expressed genes, the knockdown of *Arhgap36* in neuronal cell line HT22 significantly enhances the cell apoptosis, suggesting the impaired spatial memory induced by long-term heat stress may at least partially be mediated by the dysregulation of *Arhgap36* in hippocampal neurons. The uncovered relationship between molecular changes in the hippocampus and behavioral alterations induced by long-term heat stress may offer valuable insights for the development of therapeutic targets and protective drugs to enhance memory function in heat-exposed individuals.

1. Introduction

The escalating global average ground temperature has led to a growing apprehension regarding the risks that high-temperature heat waves pose to human populations [1,2]. The organism's normal physiological function is greatly impacted in a febrile

* Corresponding author. Department of Physiology Naval Medical University 800 Xiangyin Rd., Shanghai, 200433, PR China.
E-mail address: roadgao@163.com (L. Gao).
[1] These authors contributed equally to this work.

https://doi.org/10.1016/j.heliyon.2024.e37319
Received 4 May 2024; Received in revised form 31 August 2024; Accepted 1 September 2024
Available online 2 September 2024

environment, leading to the manifestation of pathological conditions including elevated body temperature, dehydration, gastric bleeding, and spermatogenic dysfunction [3–5]. Numerous lines of evidence indicate that heat stress significantly impacts the brain's structure and function [6,7]. For instance, delirium, confusion, and other symptoms related to the central nervous system can be attributed to heat shock in elevated temperatures [8–10]. In the context of increasing global temperatures, brain health problems due to high temperatures have attracted significant attentions worldwide [6,11].

Animal cognitive function plays a critical role in security, guidance, decision-making, and avoidance of dangerous situations [12]. Learning and memory are higher physiological activities in the brain and also the core components of cognitive function [13]. Previous studies have demonstrated that both animals and humans experience cognitive impairment as a result of exposure to high temperatures [14,15]. Furthermore, it has been observed that even mild heat stress can cause brain atrophy and cognitive deficits [16,17]. The detrimental effects of high-temperature exposure on cognitive function in experimental animals or humans have been extensively observed and confirmed [11,18]. However, there is a lack of research in simulating the effects of prolonged exposure to high-temperature environments on learning and memory function, as well as the underlying molecular regulatory mechanisms. In the current study, we established a long-term heat stress exposure model in rats and examined the changes in spatial memory and its related morphological lesions and genetic patterning in the hippocampal tissues using transcriptome sequencing analysis. It was found that spatial memory was significantly impaired in the rats undergoing long-term heat stress, with increased neuronal apoptosis at the CA3 region of hippocampus, which may be contributed by the downregulation of *Arhgap36* gene.

2. Materials and methods

2.1. Animal treatment

Adult male Sprague-Dawley rats (3 months old, 250–300 g) were purchased from Shanghai Regen Biotechnology Co., Ltd, and housed in groups of 4–6 in environmentally controlled conditions (room temperature at 20–22^{o}C, 50 % humidity, and under a 12-h light/12-h dark cycle), with free access to water and food. After a week of acclimatization, 14 rats were randomly divided into two groups with 7 rats in each group for the following 14-day experiment: Control group (CON), in which the rats were bred under room temperature and relative humidity at 50 ± 10 %; Long-term heat stress group (LTHS), in which the rats were treated daily in a constant temperature and humidity chamber (temperature 42 ± 0.5 °C, relative humidity 80 ± 10 %) for 20 min per day in 14 consecutive days [19]. The rectal temperature of rats reaching 41.5 ± 0.5 °C was considered as the successful establishment of the heat stress model [20]. To guarantee this, we optimized the settings of our experiments through multiple linear regression analysis on the rectal temperatures of 74 rats exposed to varying treatment times and temperatures, and developed a predictive model:

$$\text{Rectal temperature} = 30.287 + 0.145 \times \text{temperature} + 0.064 \times \text{relative humidity} + 0.020 \times \text{minutes}.$$

The model's coefficient of determination (R square) was calculated to be 0.743. This model revealed that at a treatment time of 20 min, a treatment temperature of 42°, and relative humidity of 80 %, the rat's rectal temperature would be approximately 41.5 °C, aligning well with our experimental findings. After heat stress treatment, rats in the LTHS group were moved back to normal conditions. All animal procedures were approved by the Animal Care and Use Committee of Naval Medical University, Shanghai (ethics approval number: 20210108005). All animal experiments were conducted in compliance with the ARRIVE guidelines (Kilkenny et al.) and adhered to the Public Health Service Policy on Humane Care and Use of Laboratory Animals.

2.2. Morris water maze

The Morris water maze is a research tool that includes a circular pool, a platform, and a video tracking system. The pool has a diameter of 210 cm and a height of 53 cm. It is divided into four quadrants, with the hidden platform located 1 cm below the water's surface in the fourth quadrant. The water temperature was maintained at 25 ± 2 °C. To enhance the visibility of rat trajectories captured by the video tracking system, the water in the pool was stained with nontoxic ink to darken the background. During the directed navigation experiment, all animals were subjected to a 4–6 day training session. In this experiment, each animal was placed in the water from four visually cued points in four quadrants. The training session continued until the rat found the hidden platform on its own or for a maximum duration of 120 s. If a rat failed to find and ascend to the hidden platform, the experimenter guided it to the platform. All experimental animals successfully ascended to the platform from the visually cued points within 4–6 days [21]. Following the application of heat stress treatment, we proceeded with the spatial exploration experiment. The platform was removed and the rats were allowed to swim freely for 60 s. Various learning and memory indexes were recorded, including the number of platform crossings, distance traveled, and escape path, for further analysis.

2.3. Histological examination of hippocampus

Following the final heat stress treatment, the rats were anesthetized using isoflurane gas and underwent cardiac perfusion with pre-chilled PBS solution, followed by 4 % paraformaldehyde. The brain tissues were then removed and fixed overnight at 4 °C in 4 % paraformaldehyde. For histological examination, sections were stained with hematoxylin solution and eosin solution for 5 min each. After staining, the sections were dehydrated, mounted, and observed under a light microscope (te2000, Nikon, Japan). Nissl staining was performed on deparaffinized sections using toluidine blue solution for 5 min, followed by differentiation in 1 % glacial acetic acid.

Subsequently, the sections were dehydrated and mounted for observation.

2.4. Immunofluorescence assay

The hippocampal specimens and cell slides were fixed with 4 % paraformaldehyde (Biosharp, BL539A), incubated with primary antibodies anti-Neuronal Nuclei (NeuN, GB15138-100, 1:500) or anti-GFAP (GB12100-100, 1:500), diluted in PBS containing 1 % bovine serum albumin (Merck, V900933) overnight at 4 °C. After three times washing with PBS, the specimens were then incubated with secondary antibody at room temperature in the dark. Following the incubation with DAPI for 10 min and a final wash, coverslips were placed on the slides which were mounted with an anti-fluorescence quenching mounting medium (Beyotime, P0126), and stored in a refrigerator at 4 °C. Analysis was conducted using a fluorescence microscope for observation and photo documentation.

2.5. TUNEL assay

The apoptosis of hippocampal neurons was assessed using the TUNEL assay (Servicebio, G1502-50T). Briefly, paraformaldehyde-fixed brain tissue samples or cell slides were treated with proteinase K, and the cell membranes were permeabilized using 0.1 % Triton for 20 min of treatment. Subsequently, the specimens were incubated with TUNEL reaction solution at room temperature for 1 h, followed by neuronal staining with NeuN and nuclei staining with DAPI. Cells displaying red fluorescence were identified as apoptotic cells, while green fluorescence indicated neuronal cells. Three fields of view were randomly selected on each slide, and the percentage of TUNEL-positive neurons was calculated.

2.6. Measurement of pituitary-related hormones

Peripheral blood from rats was collected in EP tubes sprayed with EDTA and allowed to stand at room temperature for 20 min. It was then centrifuged at 4 °C for 10 min, and the supernatant plasma was taken for ELISA detection. Commercially available rat GH, ACTH, TSH, and BDNF kits (Wuhan Servicebio Technology CO., LTD) were used to measure the levels of growth hormone (GH), adrenocorticotropic hormone (ACTH), thyroid-stimulating hormone (TSH), and brain-derived neurotrophic factor (BDNF) in the plasma. Each sample was evaluated in duplicate, and the concentration of each hormone was determined using linear regression with a standard curve.

2.7. Transcriptome sequencing

Following the final heat stress treatment, the rats were euthanized through intraperitoneal injection of a lethal dose of

Table 1
Primer list for Quantitative RT-PCR.

Gene	Primer sequence	GenBank code
arMis18a	3′-TTTGATTCCACCTCCCACAGC-5′ 5′-ACTCCCAAGAACCTGGATTACAAGA-3′	NM_001127523.2
rArhgap36	3′-GGCAAGGTGGCATCAGGTAGA-5′ 5′-CTGCGGAGGGTGATTGAGCT-3′	XM_229133.10
rGabrq	3′-CAGCGTCTCAAATGGTTGTATGG-5′ 5′-CCAGCTCATTGATGGAGGTCAT-3′	NM_031733.2
rSlc25a52	3′-AGGCACGACAGGTCCTCATACA-5′ 5′-TGCGCCGCTTTCAACAAC-3′	XM_223434.8
rMettl4	3′-CCATAGCATCCAATTCACCTCGA-5′ 5′-TCAGCCAGATCCCGTGTCTCC-3′	NM_001191814.1
rCplx3	3′-CTCCCGAGGCAGTTCCACAT-5′ 5′-GGAGCGAGACGCACAGTTCA-3′	NM_001109295.2
rScand1	3′-TGTCCGCGTCACCCTTTGT-5′ 5′-TCCGTCTTCTCCGCTTCCA-3′	NM_001108599.1
rStoml3	3′-GACAACAGCACGCTCATACTCCTTA-5′ 5′-GGCTTGAATCCCGACCCAG-3′	NM_001106431.1
rSlc26a7	3′-CGCATAAATGATGGCAGGAAACA-5′ 5′-GCACCGCAGTACAATCTGAAGG-3′	NM_001106638.1
rPdk4	3′-CAATGTGGCTTGGGTTTCCTG-5′ 5′-CATAATGTGGTCCCTACGATGGC-3′	NM_053551.2
rSlco2a1	3′-GGAGATGGTGATGATGGTGGC-5′ 5′-ACAAGTTCCTGGAGAAGCAGTATGG-3′	NM_022667.3
b*mArhgap36*	3′-CAGGCTGCTATCCTTGCTC-5′ 5′-AGTCGGTATCTTCGTTGTTTG-3′	NM_001081123.2
mGabrq	3′-CTTGTATGCCTATTCTTCGT-5′ 5′-ACATTTGCTACCACCACTT-3′	NM_001290435.1

[a] r indicates *Rattus norregicus*
[b] m indicates *Mus musculus*.

pentobarbital sodium salt solution. The brain tissues were extracted and the hippocampus was isolated from each brain sample. The hippocampi were snap-frozen in liquid nitrogen and then stored in a −80 °C freezer until transcriptome sequencing. Five samples were randomly selected from each group for transcriptome sequencing, which was performed by Shanghai Meiji Biomedical Technology Co., Ltd. Briefly, the RNA-seq transcriptome library was prepared with Illumina® Stranded mRNA Prep kit (San Diego, CA) using 1 μg of total RNA. The synthesized cDNA was subjected to end-repair, phosphorylation, and 'A' base addition according to Illumina's library construction protocol. Libraries were size selected for cDNA target fragments of 300 bp on 2 % Low Range Ultra Agarose followed by PCR amplification using Phusion DNA polymerase (NEB) for 15 cycles. The paired-end RNA sequencing library was then quantified by Qubit 4.0 and sequenced with the NovaSeq 6000 sequencer (2 × 150bp read length).

2.8. RNA extraction and RT-qPCR

Total RNA was isolated from the rat's hippocampus using TRIzol LS reagent (Thermo Fisher Scientific) and 1 μg of RNA was reverse transcribed to cDNA using the High-Capacity cDNA Reverse Transcription Kit (Applied Biosystems). Quantitative RT-PCR was performed using the SYBR green method. The GAPDH gene was used as an internal standard gene. The results were acquired after 40 cycles of amplification. The threshold cycles (Ct) were conclusive for each gene and gene expression levels were evaluated using 2–ΔΔCt. Quantification data represented the mean of triplicated experiments. Primers for each target gene were designed from primer bank, as indicated in Table 1.

2.9. HT-22 cell culture and siRNA transfection

The mouse hippocampal neuron cell line, HT-22, was obtained from the National Collection of Authenticated Cell Cultures (GNM47, Shanghai, China) and cultured in Dulbecco's modified Eagle's medium (DMEM) containing 25 mM glucose (HyClone, USA) with 10 % Fetal Bovine Serum (FBS) and 1 % penicillin-streptomycin (100 U/ml penicillin and 100 μg/ml streptomycin). The culture temperature was kept at 37 °C and the incubator atmosphere was filled with 5 % CO_2. When the cell density reached approximately 70%–80 %, passages were carried out and P2-P4 generation of cells was used for subsequent experiments. All cell lines were tested negative for any mycoplasma contamination.

Briefly, the cells were seeded into 6-well plates at a concentration of 1×10^5 cells per well. Transfection with si-Arhgap36, si-Gabrq, and their corresponding NC control (Shanghai GenePharma Company) using Lipofectamine 2000 (Invitrogen, 11668019) was performed when the HT-22 cell density reached 70 %–80 %. After 6 h of transfection, the medium was replaced with DMEM containing 10 % FBS. After another 24 h and 48 h of culture, the RNA and protein were extracted, respectively, for verification of gene silencing efficiency and subsequent experiments. Each experiment was biologically replicated 3 times.

2.10. Western blot analysis

Cell lysis was performed by treating cells with RIPA (Beyotime, P0013B) buffer containing a protease inhibitor mixture (Beyotime, P1005) on ice for 30 min, with shaking and mixing every 5 min to ensure complete lysis. Subsequently, protein quantification was carried out using the BCA assay (Beyotime, P0012S), followed by boiling the proteins in 5 × loading buffer (Beyotime, P0015) for gel electrophoresis. The prepared protein samples (20 μg) were then electrophoresed on a 10 % polyacrylamide gel with sodium dodecyl sulfate and transferred to a 0.45 μm PVDF membrane (Millipore, IPFL00010). The PVDF membrane was blocked with TBST (Epizyme, PS103) solution containing 5 % skimmed milk powder for 2 h, followed by overnight incubation with primary antibodies for procaspase-3 (9662S, 1:1000), cleaved caspase-3 (9662S, 1:1000) and α-tubulin (2144S, 1:1000) at 4 °C. After three times washing with TBST, the membrane was then incubated with either goat anti-rabbit (Proteintech, RGAR006) or goat anti-mouse (Proteintech, RGAM006) immunoglobulin G (IgG) horseradish peroxidase secondary antibody for 2 h at room temperature, followed by three times washing with TBST. Immunoreactive bands were visualized using chemiluminescence with an ECL kit (Epizyme, SQ202), and protein intensity was quantified using ImageJ software.

2.11. Flow cytometry

HT22 cell apoptotic rate was determined using flow cytometry with a FITC-Annexin V/PI kit (Beyotime, C1062S). After 48 h of siRNA transfection, the HT22 cells were digested with 0.25 % trypsin (Gibco, R001100), centrifuged to eliminate the culture medium, and subsequently reconstituted in 500 μl of 1 × Binding Buffer after rinses with PBS. Annexin V FITC and PI (5 μl each) were added to individual cell tubes, mixed gently, and incubated at room temperature in the dark for 15 min. Apoptosis was analyzed by a BD FACSCalibur flow cytometer (BD Bioscience, USA) and analyzed with FlowJo software (TreeStar, Ashland, Ore).

2.12. Statistical analysis

All experimental data were expressed as mean ± SEM. To determine significance, data were subjected to unpaired Student's t-test using Graphpad Prism software statistical package 9 (Graphpad software). The criterion for significance was set at $P \leq 0.05$.

3. Results

3.1. Long-term heat stress impairs spatial memory function in rats

To determine whether HS could affect the learning and memory function of rats, the Morris water maze (MWM) test was employed. Both the control and HS group rats participated in a four-day directional navigation experiment before the heat stress treatment. Following the long-term heat stress treatment, which lasted for 14 days, a spatial exploration experiment was conducted (Fig. 1A). There are no significant differences in escape latency in the hidden platform between the control group and the heat-treated group (Fig. 1B), suggesting that the spatial learning ability of the rats in both groups was comparable before the long-term heat stress. In the spatial exploration experiment, the rats in the heat stress group manifested a significant decrease in the distance traveled and time spent around the platform (Fig. 1C–E), as well as a lower number of times crossing the platform (Fig. 1F), in comparison to the rats in the control group. However, there was no significant difference in swim speed between the two groups (Fig. 1G), indicating that the motor abilities of rats were not impaired by long-term heat stress.

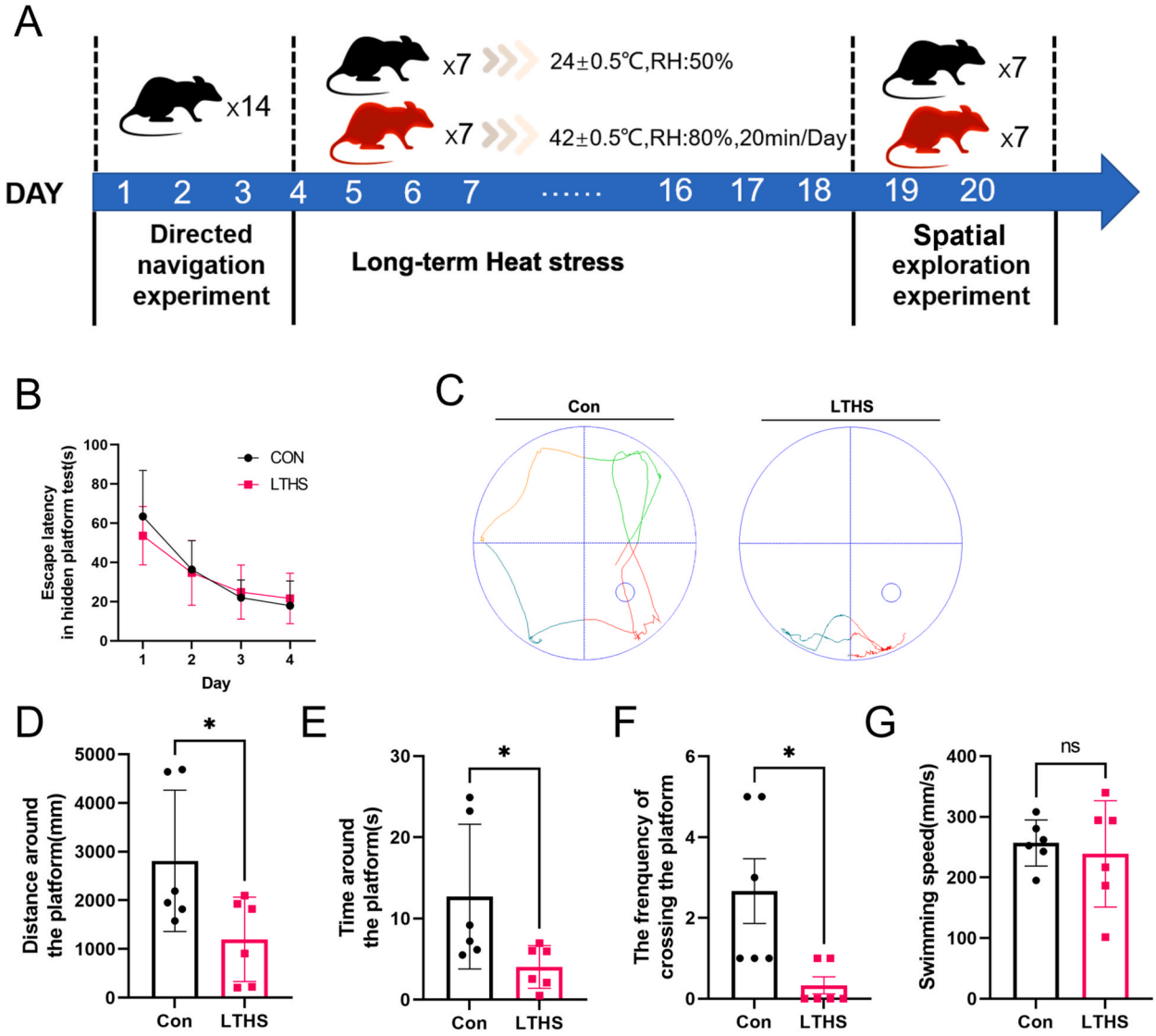

Fig. 1. Spatial memory functions of rats determined by Morris water maze. (A) Processing mode diagram. (B) Escape latency periods of different groups in the directional navigation experiment. (C) Representative images of typical moving trajectory in the probe trial. (D) Swimming distance around the platform. (E) Traveling time around the platform. (F) The frequency of crossing the platform. (G) Swimming speed. Unpaired Student's t-test was applied as the statistical method. The data are presented as the mean ± SEM (n = 6 for each group). LTHS: long-term heat stress. *p < 0.05, versus the control group. ns: non-significant.

3.2. Long-term heat stress causes pathological damage to hippocampal neurons

Learning and memory functions are intricately linked to the hippocampus region of the brain. To gain a deeper understanding of how rats experience impaired memory function under long-term heat stress, we examined the morphological changes in hippocampal neurons. It can be seen that the number of normal neurons in the CA3 region of the hippocampus from LTHS rats significantly decreased compared to the control group. The normal structure of neurons is difficult to discern, and apparent karyopyknosis can be observed in the neurons of the CA3 region of the hippocampus from LTHS rats (Fig. 2A and C). The Nissl body is a basophilic iron-containing nucleic acid protein that serves as the main site for protein synthesis in neurons. Normally, Nissl bodies appear as large or granular particles surrounding the nucleus, with variations in size and elongation towards the edge. These characteristics allow for the observation of neuronal morphology and functional status. Our results also demonstrated that in the LTHS group, Nissl bodies in the CA3 hippocampal neurons exhibited dramatically deeper staining, compared to that in the control group (Fig. 2A). However, the number of neurons and morphology of nuclei manifested no significant abnormity in both CA1 and DG regions of hippocampus from LTHS rats (Supplementary Figs. 1A–1B). These structural damages observed in neurons indicated that heat stress might have triggered abnormal initiation of programmed cell death. Consequently, we employed immunofluorescence techniques to stain and analyze apoptotic signals alongside the neuronal marker Neuronal Nuclei (NeuN) in hippocampal specimens. The findings revealed a decrease in neuronal signals within the CA3 region of the LTHS group, along with a dramatically increased expression of apoptotic signals in the affected areas within the CA3 region (Fig. 2B and D). In essence, exposure to heat stress led to an increase in neuronal apoptosis specifically in the CA3 region of the hippocampal tissue, since no significant changes in neuronal signals or apoptotic signals were observed in the CA1 or DG regions (Supplementary Figs. 1C–1D).

To further dissect if the LTHS also causes the damage on astrocytes in the hippocampus, we stained and analyzed apoptotic signals alongside the astrocyte marker glial fibrillary acidic protein (GFAP) in hippocampal specimens, and found that neither the number of GFAP-positive astrocytes nor the apoptotic signals manifested significant alterations in CA1, CA3 and DG regions between LTHS group and control group (Supplementary Figs. 2A–2C).

Since previous studies showed that some pituitary hormones have potential neuroprotection effects on cognitive dysfunction against heat stress, we further determined the levels of growth hormone (GH), adrenocorticotropic hormone (ACTH), thyroid

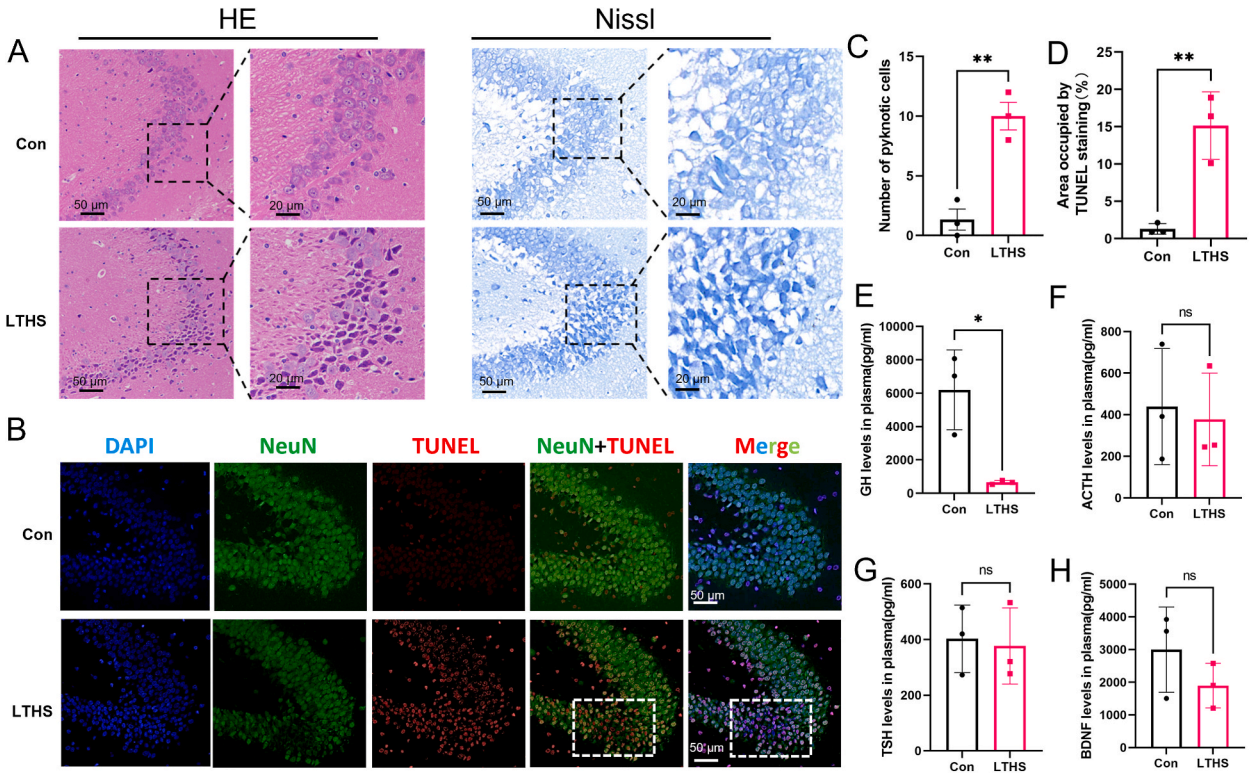

Fig. 2. Morphological changes of rat hippocampal neurons at CA3 regions and the levels of pituitary hormones. (A) Representative HE staining and Nissl staining of CA3 regions in rat hippocampal tissues. (B) Immunofluorescence staining of normal and apoptotic neurons in CA3 region. (C) The percentage of neurons that occurred karyopyknosis in CA3 regions. (D) The percentage of TUNEL-positive neurons in CA3 regions. (E–H) The plasma levels of GH, ACTH, TSH, and BDNF in peripheral blood of rats. NeuN: neuronal nuclei, GH: growth hormone, ACTH: adrenocorticotropic hormone, TSH: thyroid stimulating hormone, BDNF: brain-derived neurotrophic factor. Unpaired Student's t-test was applied as the statistical method. The data are presented as the mean ± SEM (n = 3). *p < 0.05, **p < 0.01 versus the control group. ns: non-significant. Scale bars are indicated in each panel of the figure.

stimulating hormone (TSH) and brain-derived neurotrophic factor (BDNF) in the peripheral blood of rats, and found that only the level of GH but no other pituitary hormones was significantly decreased by the prolonged heat stress (Fig. 2E–H).

3.3. RNA transcriptome sequencing reveals the main pathways and differentially expressed genes in hippocampal tissues upon heat stress

By analyzing the transcriptome sequencing results of hippocampal tissues, we identified a total of 179 differentially expressed genes (DEGs) that met the criteria of log2FoldChange absolute value ≥ 1 and P value ≤ 0.05 (Fig. 3A). Among them, 86 genes were up-regulated while 93 genes were down-regulated in the LTHS group compared to the control group, respectively (Fig. 3B–Supplementary Table 1). To investigate the functional association of these genes, we performed GO and KEGG analyses. The KEGG enrichment analysis revealed significant down-regulation in the regulation of biological stimulation response, positive regulation of external stimulation response, and regulation of innate immune response in the heat stress group (Fig. 3C), which were further supported by the GO enrichment analysis (Fig. 3D). These findings suggested that heat stress treatment may negatively impact spatial memory function by inhibiting the normal stress stimulation response and immune response in hippocampal tissues.

3.4. Verification of differentially expressed genes

To verify the RNA-seq data, all differentially expressed genes with log2FoldChange absolute values greater than 1.2 and P values less than 0.05 were selected (Fig. 4A) and their expression was verified using qRT-PCR. Consistent with the RNA-seq data, the mRNA levels of Arhgap36, Gabrq, and Mettl4, showed a significant reduction in heat-stressed hippocampal tissues compared to the control hippocampus (Fig. 4B–D). The mRNA levels of Slco2a1, Cplx3, and Stoml3 were significantly increased in heat-stressed hippocampal tissues compared to the control hippocampus (Fig. 4E–G). However, there were no significant differences in the mRNA levels of other selected genes, such as Scand1, Slc25a52, Pdk4, Mis18a, and Slc26a7, which are inconsistent with the results from the RNA-seq data (Supplementary Figs. 3A–3E).

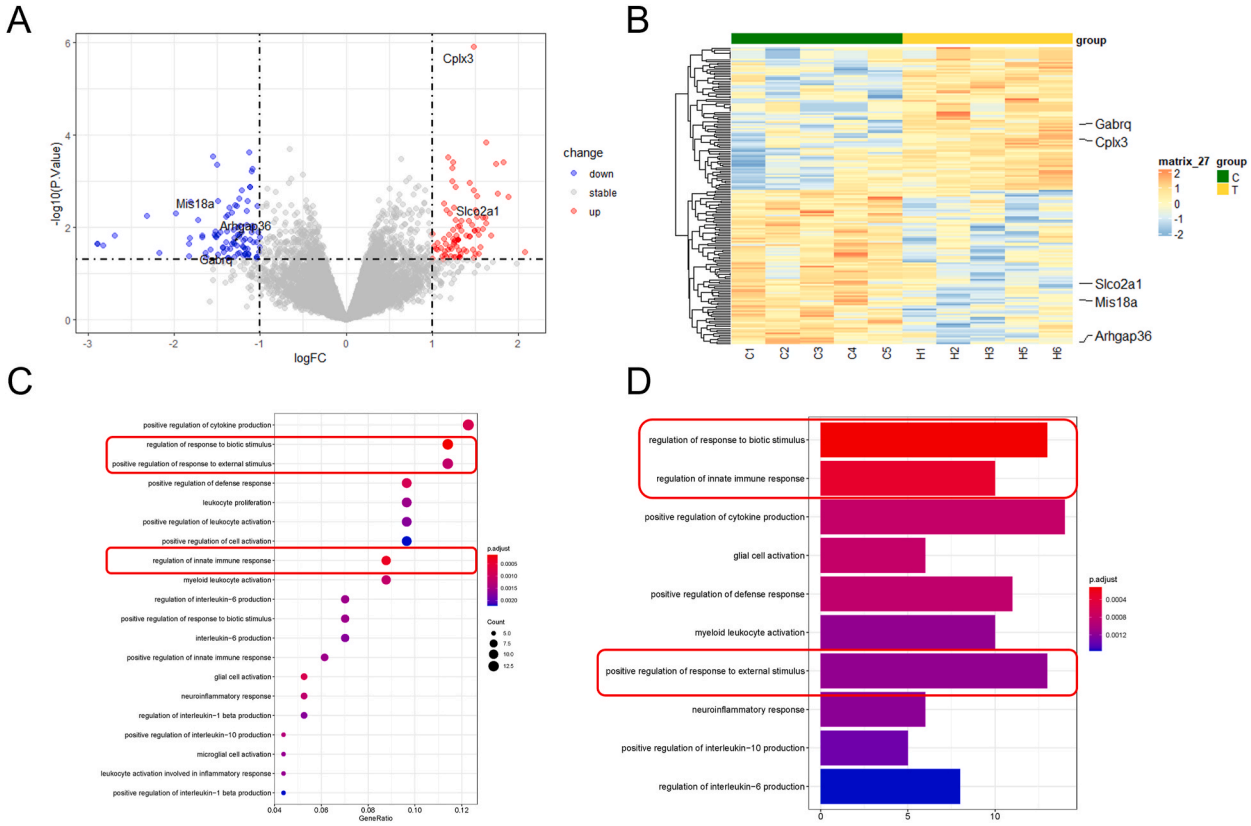

Fig. 3. Differentially expressed genes and related pathways enrichment in hippocampal tissues upon heat stress. (A) The volcano Plot shows the differentially expressed genes (DEGs). (B) Heat map for DEGs. (C) KEGG pathways enrichment analysis with DEGs. (D) GO enrichment analysis with DEGs.

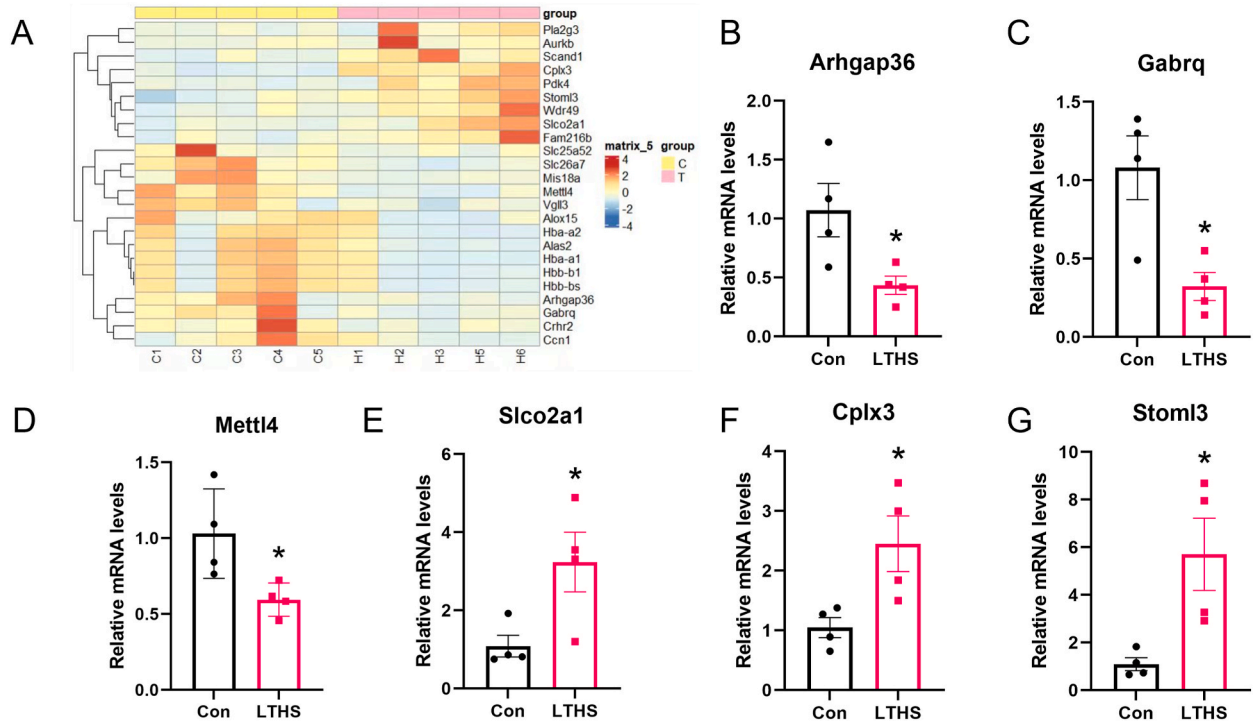

Fig. 4. Verification of DEGs revealed by RNA Sequencing. (A) Heat map of the DEGs with log2FoldChange absolute values greater than 1.2 and P values less than 0.05. The mRNA expression of *Arhgap36* (B), *Gabrq* (C), *Mettl4* (D), *Slco2a1* (E), *Cplx3* (F), and *Stoml3* (G) were measured by RT-qPCR. Unpaired Student's t-test was applied as the statistical method. The data are presented as the mean ± SEM (n = 4 for each group). *p < 0.05 versus the control group.

3.5. *Knockdown of Arhgap36 can lead to increased apoptosis of hippocampal neurons*

To further investigate the functional roles of *Arhgap36* and *Gabrq* in the response to LTHS-induced hippocampal impairment, we knocked down the expression of *Arhgap36* and *Gabrq* in the mouse hippocampal neuron cell line HT-22 using their specific siRNAs. After 48 h of transfection, it was found that the mRNA expression of *Arhgap36* was significantly decreased in HT-22 cells (Supplementary Fig. 4A). The expression of cleaved caspase 3 was significantly increased in the HT-22 cells that *Arhgap36* was knocked down (Fig. 5A and B), indicating the downregulation of *Arhgap36* enhances the apoptotic levels of HT-22 cells. The TUNEL assay and flow cytometry analysis also showed consistent results that the apoptotic levels of HT-22 cells were dramatically increased upon *Arhgap36* knockdown (Fig. 5C and D). On the contrary, the knockdown of *Gabrq* (Supplementary Fig. 4A) did not affect the apoptotic levels of HT-22 cells (Supplementary Figs. 4B–4E).

3.6. *Discussion*

Heat stress can lead to various physiological and pathophysiological changes in the body. In recent years, researchers have become increasingly interested in understanding the impact of heat stress on the central nervous system's functions and tissue structure, as brain science research progresses [22–25]. While many scholars have explored the effects of heat stress on learning and memory functions using experiments like MWM, the underlying molecular mechanism remains unclear [26–28]. It has been reported that heat stress can lead to memory dysfunction in mice by influencing the process of neurogenesis [8]. However, the potential impact of heat stress on memory function through mechanisms such as neuronal apoptosis and other related processes remains unexplored. Identifying the key targets through which heat stress affects spatial memory function can provide a foundation for medical support in high-temperature environments due to global warming. By conducting MWM tests, we observed impaired spatial memory function in heat-stressed rats. The HE, Nissl, and TUNEL staining indicated that LTHS causes karyopyknosis damage to hippocampal neurons due to increased neuronal apoptosis specifically at the CA3 region, other than CA1 and DG regions. The CA3 region of the hippocampus is important for rapid and precise encoding of memory [29,30], while the CA1 region is necessary for retrieving the gist of events and for recalling the most remote memories [30]. Since our setting of experiments only determined the changes in rapid memory functions, our findings are consistent with these previous reports and suggest that only the rapid memory function was affected by the LTHS treatment due to the pathological damage at the CA3 region, while the remote and lifetime memory may not be influenced by the LTHS with the relatively unaffected CA1 region in the hippocampus. The DG region, known for housing neurons with differentiation potential [31–34], is not significantly damaged by LTHS either, suggesting that the spatial memory is potential to be recovered upon

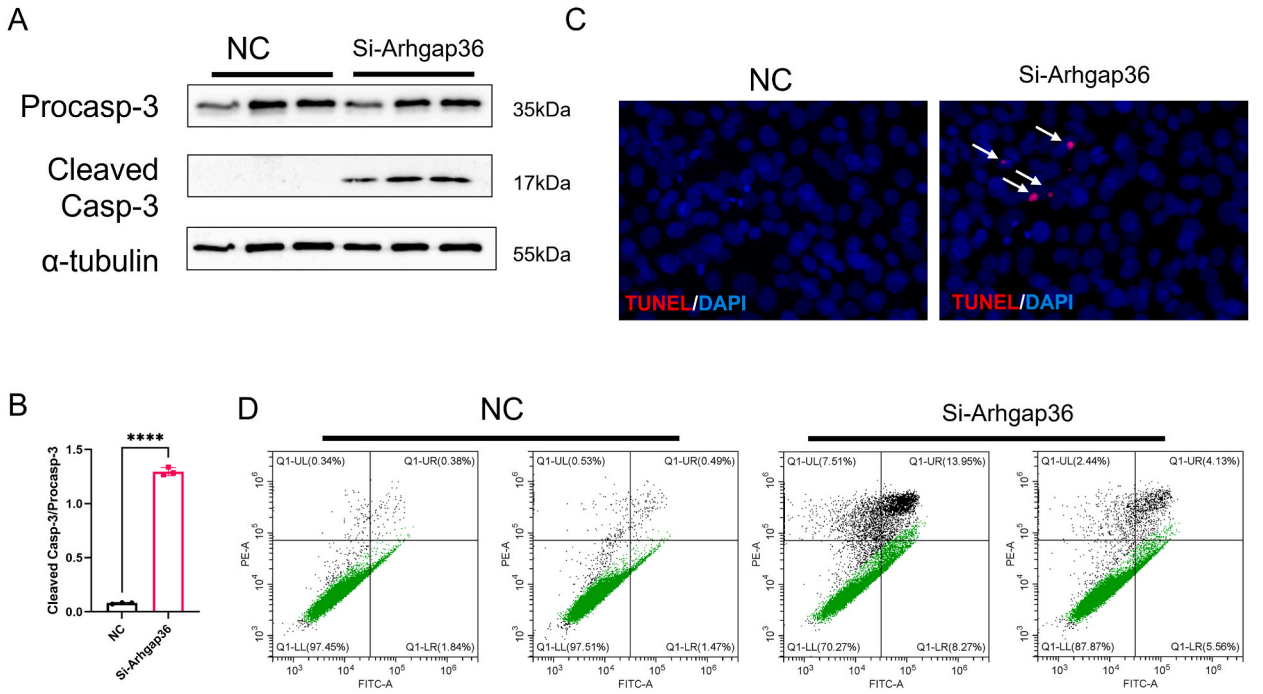

Fig. 5. Apoptosis of HT-22 cells after knockdown of *Arhgap36*. (A) Expression levels of apoptosis-related protein cleaved-Caspase3 in NC group and *Arhgap36* knockdown group. (B) Densitometric quantitation of cleaved caspase-3 relative to pro-caspase-3. The data are presented as the mean ± SEM (n = 3 for each group). ****$p < 0.0001$, versus the NC group. (C) The representative image for TUNEL staining of HT-22 cells after *Arhgap36* was knocked down. (D) The representative image of flow cytometry for detecting the HT-22 cell apoptosis.

removal from the detrimental heat stress. Interestingly, we also observed that the level of GH in peripheral blood was significantly decreased upon LTHS. GH is well known to regulate somatic growth and metabolic processes. However, recent observations suggest that GH is also involved in regulating brain growth, development, and myelination, as well as influencing cognitive behavior and higher nervous activity through the modulation of other neurotransmitters [35]. Previous studies show that topical application of GH induces pronounced neuroprotective effects following spinal cord injury [36]. These neuroprotective effects of GH may be attributed either to circulating insulin-like growth factor-1 (IGF-1) or to locally produced IGF-1 within the brain [37]. GH influences signal transductions in the microvessels as well. Thus, GH-induced IGF-1 increases progenitor cell proliferation through mitogen-activated protein kinase signaling pathways and exerts antiapoptotic effects through PI3-K/Akt or mitogen-activated protein (MAP) kinase/Erk signaling in adult brains [23]. Our results, combined with previously reported neuroprotective effects of GH on heat stress-induced cognitive dysfunction and brain pathology [23,25], suggest that GH might be a critical hormone to normal morphology and function of the hippocampus whereas the deficits of GH induced by LTHS may contribute to the damage of hippocampal neurons and spatial memory functions.

To investigate the genetic patterning associated with LTHS-induced spatial memory impairment, we conducted RNA-sequencing using the hippocampal tissues of rats from both the control group and LTHS groups. Through a combination of GO and KEGG pathway enrichment analyses, we revealed a notable down-regulation of biological stress and external stress response pathways in the hippocampal tissue from the LTHS group. To our knowledge, it is the first time to reveal the genetic patterning in the hippocampus of rats undergoing long-term heat stress treatment.

In the major downregulated pathways, the expression of *Arhgap36* and *Gabrq* is verified to be significantly decreased in hippocampal tissues of heat-stressed rats, which is consistent with RNA- RNA-sequencing data. *Arhgap36* encodes a putative Rho GTPase-activating protein ARHGAP36, which is identified as a positive regulator of the Sonic hedgehog (Shh) pathway [38]. Through the combination of animal models and *in vitro* loss-of-function experiments, we found that the expression of *Arhgap36* in hippocampal tissue decreases post heat stress, consequently leading to an increase in the proportion of hippocampal neuron apoptosis. These results suggested that *Arhgap36* is a target gene at least partially responsible for the structural damage to hippocampal neurons induced by LTHS. Although the specific signal transduction pathways bridging the effects of ARHGAP36 and apoptosis remain unclear, our research lays a foundation for understanding the impact of adverse environmental factors on the central nervous system. ARHGAP36 has emerged as a potent antagonist of PKA signaling by interacting with catalytic subunits of PKA (PKAC) and inhibits the catalytic activity of PKA [39]. Recent studies in cultured cells suggest that ARHGAP36 regulates Shh activity by inhibiting PKA kinase activity [40]. Seunghee Lee et al. found that the ARHGAP36 functions as an essential effector of Shh and AKT in the generation of motor neurons in the spinal cord [41]. Due to the crucial roles of the Shh pathway in cell proliferation, differentiation, and ontogeny, it is of great interest to dissect if the specific effect of *Arhgap36* on the apoptosis of hippocampal neurons is mediated by the PKA-Shh pathway

in the future study.

Gabrq encodes gamma-aminobutyric acid type A (GABAA) receptor subunit theta (GABRQ), which is a crucial subunit of the GABAA receptor in the mammalian brain [42]. GABA-mediated synaptic depression plays a critical role in normal neural functioning [43], and research has shown that abnormalities in GABAA receptor subunits can contribute to various central nervous system disorders, including anxiety disorders, epilepsy, schizophrenia, and insomnia [44–46]. The proper expression of GABAA receptor subunits is also closely linked to learning and memory functions [47–49]. Studies conducted in mice have demonstrated that knock-out of the Gabrq upstream transcriptional factor Egr-1 leads to a significant decrease in the expression of GABRQ and other GABA receptor subunits in the hippocampal tissue, resulting in long-term spatial memory impairment [50]. Although we didn't observe the effects of *Gabrq* knockdown on the apoptosis of hippocampal neurons in *in vitro* experiments, it cannot be excluded the possibility that LTHS-reduced GABRQ may influence the learning and memory functions of rats through other pathways.

4. Conclusion

In the current study, we reveal that long-term heat stress causes impaired spatial memory in rats due to morphological damage and apoptosis of hippocampal neurons at the CA3 region, which may be mediated by the decreased expression of *Arhgap36*, accompanied by a decrease in growth hormone levels in peripheral blood. Future studies are warranted to observe if the restoration of ARHGAP36 rescues the spatial memory damage induced by LTHS, which will provide more confidence to develop new strategies for spatial memory protection from detrimental environmental factors.

Fundings

National Key Research and Development Project 2022YFC2704602 and 2022YFC2704502, National Natural Science Foundation of China 82120108011 and 82371699, Major Project of Shanghai Municipal Education Commission Scientific Research and Innovation Plan 2021-01-07-00-07-E00144, and Strategic Collaborative Research Program of the Ferring Institute of Reproductive Medicine FIRMA200502.

Disclosure and competing interests statement

The authors declare that they have no competing interests relating to this work.

Data availability

The dataset produced in this study is available in the following database:RNA-Seq Data: https://www.ncbi.nlm.nih.gov/bioproject/PRJNA1036416.

CRediT authorship contribution statement

Peihua Long: Writing – original draft, Project administration, Methodology, Formal analysis, Data curation, Conceptualization. **Qunfei Ma:** Investigation. **Zhe Wang:** Visualization, Software. **Guanqin Wang:** Validation. **Jianan Jiang:** Validation. **Lu Gao:** Writing – review & editing, Project administration, Funding acquisition.

Declaration of competing interest

The authors declare that they have no known competing financial interests or personal relationships that could have appeared to influence the work reported in this paper.

Appendix A. Supplementary data

Supplementary data to this article can be found online at https://doi.org/10.1016/j.heliyon.2024.e37319.

References

[1] A. Bonell, et al., Environmental heat stress on maternal physiology and fetal blood flow in pregnant subsistence farmers in the Gambia, west Africa: an observational cohort study, Lancet Planet. Health 6 (12) (2022) e968–e976.
[2] S.A. Lewandowski, J.L. Shaman, Heat stress morbidity among US military personnel: daily exposure and lagged response (1998-2019), Int. J. Biometeorol. 66 (6) (2022) 1199–1208.
[3] P. Habibi, et al., Effect of heat stress on DNA damage: a systematic literature review, Int. J. Biometeorol. 66 (11) (2022) 2147–2158.
[4] F. Zhao, et al., Melatonin alleviates heat stress-induced oxidative stress and apoptosis in human spermatozoa, Free Radic. Biol. Med. 164 (2021) 410–416.
[5] A. Bouchama, E.B. De Vol, Acid-base alterations in heatstroke, Intensive Care Med. 27 (4) (2001) 680–685.

[6] K. Nakamura, Y. Nakamura, N. Kataoka, A hypothalamomedullary network for physiological responses to environmental stresses, Nat. Rev. Neurosci. 23 (1) (2022) 35–52.
[7] I. Alsharif, Comprehensive exploration of the molecular response, clinical signs, and histological aspects of heat stress in animals, J. Therm. Biol. 110 (2022) 103346.
[8] W. Lee, et al., Heat stress-induced memory impairment is associated with neuroinflammation in mice, J. Neuroinflammation 12 (2015) 102.
[9] Z. Yan, et al., Combined exposure of heat stress and ozone enhanced cognitive impairment via neuroinflammation and blood brain barrier disruption in male rats, Sci. Total Environ. 857 (Pt 3) (2023) 159599.
[10] M. Moon, et al., Coptidis rhizoma prevents heat stress-induced brain damage and cognitive impairment in mice, Nutrients 9 (10) (2017).
[11] X. Zhu, et al., Effect of heat stress on hippocampal neurogenesis: insights into the cellular and molecular basis of neuroinflammation-induced deficits, Cell. Mol. Neurobiol. 43 (1) (2023).
[12] A.J. Porcelli, et al., The effects of acute stress on human prefrontal working memory systems, Physiol. Behav. 95 (3) (2008) 282–289.
[13] M. Liguz-Lecznar, G. Dobrzanski, M. Kossut, Somatostatin and somatostatin-containing interneurons-from plasticity to pathology, Biomolecules 12 (2) (2022).
[14] T. McMorris, et al., Heat stress, plasma concentrations of adrenaline, noradrenaline, 5-hydroxytryptamine and cortisol, mood state and cognitive performance, Int. J. Psychophysiol. 61 (2) (2006) 204–215.
[15] J.J. Kim, D.M. Diamond, The stressed hippocampus, synaptic plasticity and lost memories, Nat. Rev. Neurosci. 3 (6) (2002) 453–462.
[16] J. Huang, et al., β-Hydroxybutyric acid attenuates heat stress-induced neuroinflammation via inhibiting TLR4/p38 MAPK and NF-κB pathways in the hippocampus, FASEB J 36 (4) (2022) e22264.
[17] M. Erfani, , et al.L. Rosa canina, Methanolic extract prevents heat stress-induced memory dysfunction in rats, Exp. Physiol. 104 (10) (2019) 1544–1554.
[18] N.R. Chauhan, et al., Heat stress induced oxidative damage and perturbation in BDNF/ERK1/2/CREB axis in hippocampus impairs spatial memory, Behav. Brain Res. 396 (2021) 112895.
[19] J. Mahmoudi, et al., Sericin alleviates thermal stress induced anxiety-like behavior and cognitive impairment through regulation of oxidative stress, apoptosis, and heat-shock protein-70 in the Hippocampus, Neurochem. Res. 46 (9) (2021) 2307–2316.
[20] A. Gupta, et al., Heat precondition is a potential strategy to combat hepatic injury triggered by severe heat stress, Life Sci. 269 (2021) 119094.
[21] M. ElSaadani, et al., Post-traumatic brain injury antithrombin III recovers Morris water maze cognitive performance, improving cued and spatial learning, J. Trauma Acute Care Surg. 91 (1) (2021) 108–113.
[22] T. Yamaguchi, et al., Effect of heat stress on blood-brain barrier integrity in iPS cell-derived microvascular endothelial cell models, PLoS One 14 (9) (2019) e0222113.
[23] D.F. Muresanu, H.S. Sharma, Chronic hypertension aggravates heat stress induced cognitive dysfunction and brain pathology: an experimental study in the rat, using growth hormone therapy for possible neuroprotection, Ann. N. Y. Acad. Sci. 1122 (2007).
[24] S.D. Ginsberg, et al., The penalty of stress - epichaperomes negatively reshaping the brain in neurodegenerative disorders, J. Neurochem. 159 (6) (2021) 958–979.
[25] D.F. Muresanu, A. Sharma, H.S. Sharma, Diabetes aggravates heat stress-induced blood-brain barrier breakdown, reduction in cerebral blood flow, edema formation, and brain pathology: possible neuroprotection with growth hormone, Ann. N. Y. Acad. Sci. 1199 (2010) 15–26.
[26] G. Sun, et al., Aircraft noise, like heat stress, causes cognitive impairments via similar mechanisms in male mice, Chemosphere 274 (2021) 129739.
[27] Z. Su, et al., Heat stress preconditioning improves cognitive outcome after diffuse axonal injury in rats, J. Neurotrauma 26 (10) (2009) 1695–1706.
[28] J. Liu, et al., Dysfunction of iron metabolism and iron-regulatory proteins in the rat Hippocampus after heat stroke, Shock 51 (6) (2019) 780–786.
[29] N. Rebola, M. Carta, C. Mulle, Operation and plasticity of hippocampal CA3 circuits: implications for memory encoding, Nat. Rev. Neurosci. 18 (4) (2017) 208–220.
[30] E. Atucha, et al., Recalling gist memory depends on CA1 hippocampal neurons for lifetime retention and CA3 neurons for memory precision, Cell Rep. 42 (11) (2023) 113317.
[31] J. Stefani, et al., Disruption of the microglial ADP receptor P2Y13 enhances adult hippocampal neurogenesis, Front. Cell. Neurosci. 12 (2018) 134.
[32] J. Wang, et al., FOXG1 contributes adult hippocampal neurogenesis in mice, Int. J. Mol. Sci. 23 (23) (2022).
[33] T. Zhang, et al., Akt3-mTOR regulates hippocampal neurogenesis in adult mouse, J. Neurochem. 159 (3) (2021) 498–511.
[34] Z. Xia, et al., Fe3O4 nanozymes improve neuroblast differentiation and blood-brain barrier integrity of the hippocampal dentate gyrus in D-galactose-induced aged mice, Int. J. Mol. Sci. 23 (12) (2022).
[35] N.D. Aberg, K.G. Brywe, J. Isgaard, Aspects of growth hormone and insulin-like growth factor-I related to neuroprotection, regeneration, and functional plasticity in the adult brain, Sci. World J. 6 (2006) 53–80.
[36] F. Nyberg, H.S. Sharma, Repeated topical application of growth hormone attenuates blood-spinal cord barrier permeability and edema formation following spinal cord injury: an experimental study in the rat using Evans blue, ([125])I-sodium and lanthanum tracers, Amino Acids 23 (1–3) (2002) 231–239.
[37] J.O. Jørgensen, et al., Pulsatile versus continuous intravenous administration of growth hormone (GH) in GH-deficient patients: effects on circulating insulin-like growth factor-I and metabolic indices, J. Clin. Endocrinol. Metabol. 70 (6) (1990) 1616–1623.
[38] P.G. Rack, et al., Arhgap36-dependent activation of Gli transcription factors, Proc. Natl. Acad. Sci. U. S. A. 111 (30) (2014) 11061–11066.
[39] R.L. Eccles, et al., Bimodal antagonism of PKA signalling by ARHGAP36, Nat. Commun. 7 (2016) 12963.
[40] B. Zhang, et al., Patched1-ArhGAP36-PKA-Inversin axis determines the ciliary translocation of Smoothened for Sonic Hedgehog pathway activation, Proc. Natl. Acad. Sci. U. S. A. 116 (3) (2019) 874–879.
[41] H. Nam, et al., Critical roles of ARHGAP36 as a signal transduction mediator of Shh pathway in lateral motor columnar specification, Elife 8 (2019).
[42] E. García-Martín, et al., Gamma-aminobutyric acid (GABA) receptors GABRA4, GABRE, and GABRQ gene polymorphisms and risk for migraine, J. Neural. Transm. 125 (4) (2018) 689–698.
[43] W. Chen, et al., Distinct functional alterations and therapeutic options of two pathological de novo variants of the T292 residue of GABRA1 identified in children with epileptic encephalopathy and neurodevelopmental disorders, Int. J. Mol. Sci. 23 (5) (2022).
[44] S.Y. Bando, et al., Transcriptomic analysis reveals distinct adaptive molecular mechanism in the hippocampal CA3 from rats susceptible or not-susceptible to hyperthermia-induced seizures, Sci. Rep. 13 (1) (2023) 10265.
[45] A.A. Dijkstra, et al., Von economo neurons and fork cells: a neurochemical signature linked to monoaminergic function, Cerebr. Cortex 28 (1) (2018) 131–144.
[46] C.M. Davenport, et al., Relocation of an extrasynaptic GABAA receptor to inhibitory synapses freezes excitatory synaptic strength and preserves memory, Neuron 109 (1) (2021).
[47] G. Chapouthier, P. Venault, GABA-A receptor complex and memory processes, Curr. Top. Med. Chem. 2 (8) (2002) 841–851.
[48] C.F. Heaney, J.W. Kinney, Role of GABA(B) receptors in learning and memory and neurological disorders, Neurosci. Biobehav. Rev. 63 (2016).
[49] D.H. Kim, et al., Roles of GABAA receptor α5 subunit on locomotion and working memory in transient forebrain ischemia in mice, Prog. Neuro-Psychopharmacol. Biol. Psychiatry 102 (2020) 109962.
[50] J. Mo, et al., Early growth response 1 (Egr-1) directly regulates GABAA receptor α2, α4, and θ subunits in the hippocampus, J. Neurochem. 133 (4) (2015) 489–500.